Electronic Supplementary Material (ESI) for Journal of Materials Chemistry A.

<Supplementary Information>

Atomically Miniaturized Bi-Phase IrO_x/Ir Catalysts Dotted on N-doped Carbon Nanotubes for High-Performance Li-CO_2 Batteries

*Yeo-Jin Rho,[‡a] Boran Kim,[‡a] Kihyun Shin,[‡b] Graeme Henkelman[b], and Won-Hee Ryu[*a]*

[a] Department of Chemical and Biological Engineering, Sookmyung Women's University, 100 Cheongpa-ro 47-gil, Yongsan-gu, Seoul 04310, Republic of Korea.

[b] Department of Chemistry and the Oden Institute for Computational Engineering and Science, The University of Texas at Austin, Austin, Texas 78712-1224, United States

‡ These authors contributed equally to this work

Corresponding author: whryu@sookmyung.ac.kr (W.-H. Ryu)

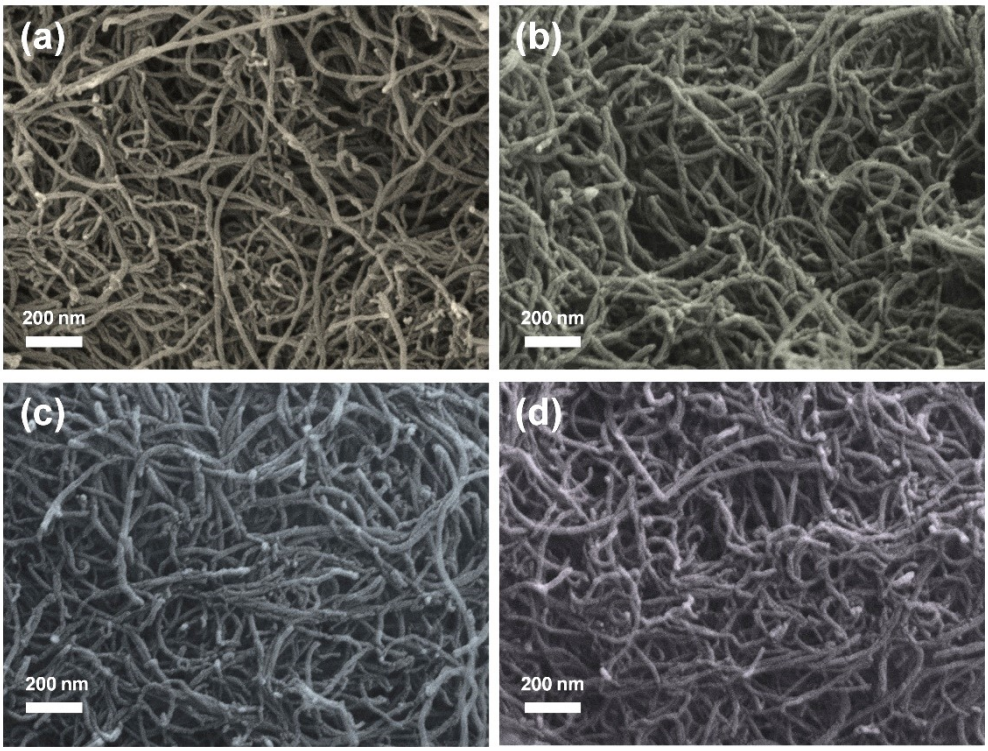

Figure S1. SEM images of (a) NCNT, (b) s-Ir/NCNT, (c) m-Ir/NCNT, and (d) l-Ir/NCNT.

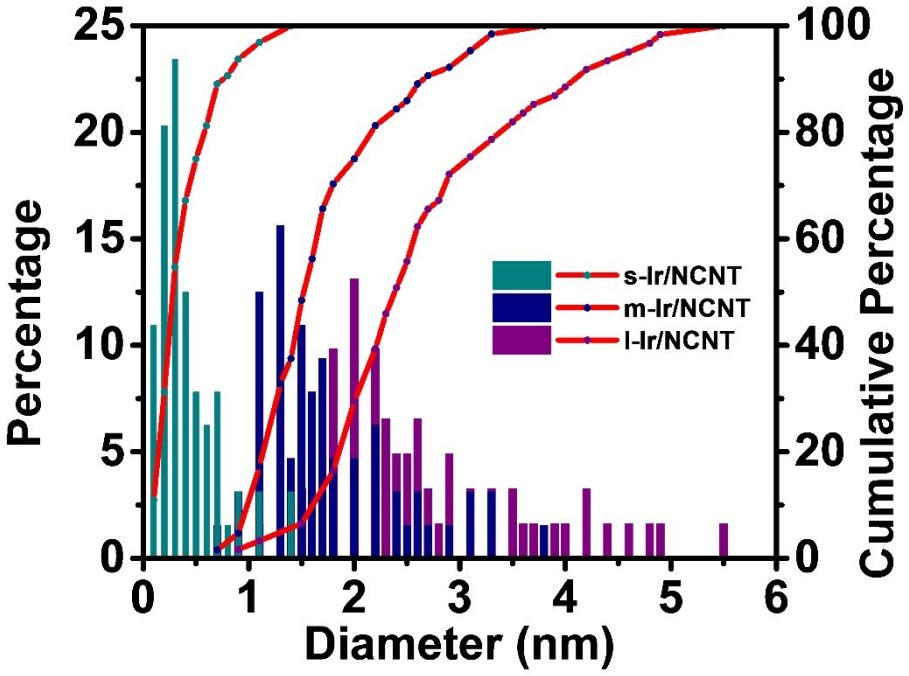

Figure S2. Size distribution of s-, m- and l-Ir/NCNTs.

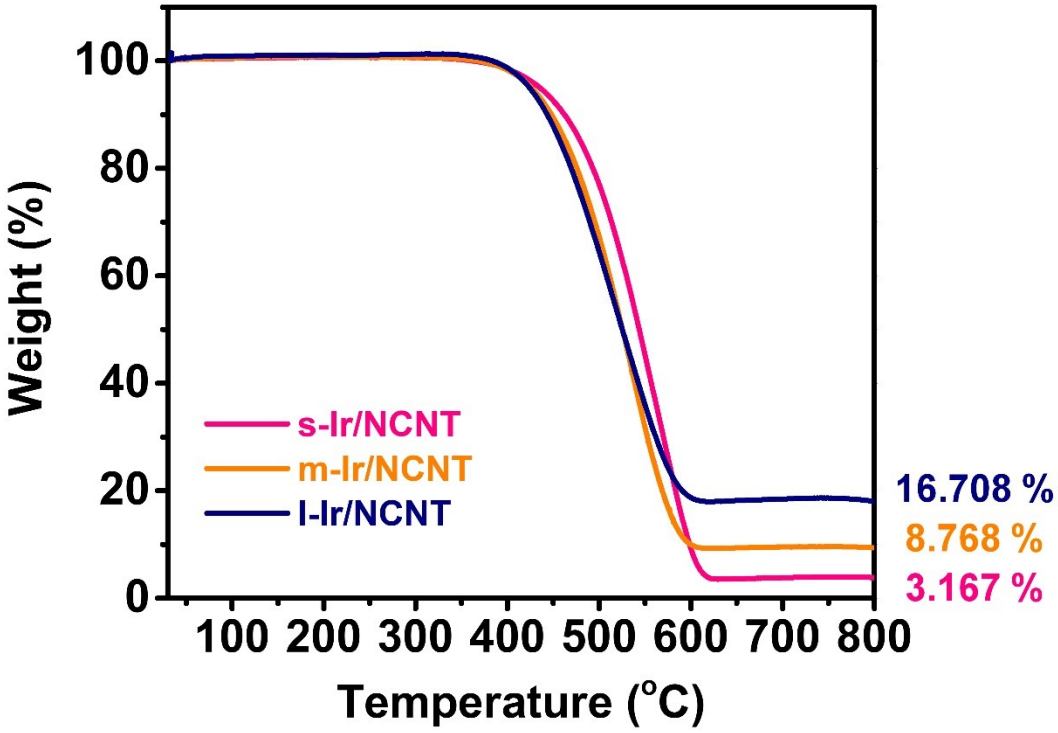

Figure S3. TGA curves of s-, m- and l-Ir/NCNTs in the temperature range of 30–800 °C at a heating rate of 10 °C/min in air.

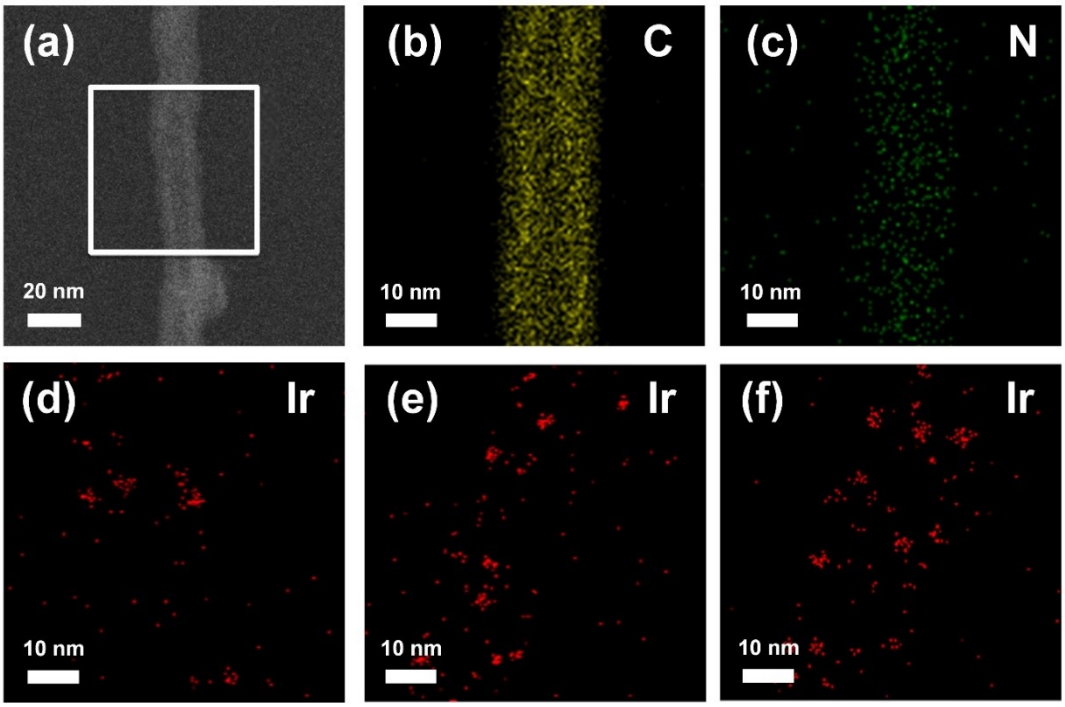

Figure S4. (a) STEM image and EDS mappings of (b) C and (c) N in NCNT and Ir in (d) s-Ir/NCNT, (e) m-Ir/NCNT and (f) l-Ir/NCNT.

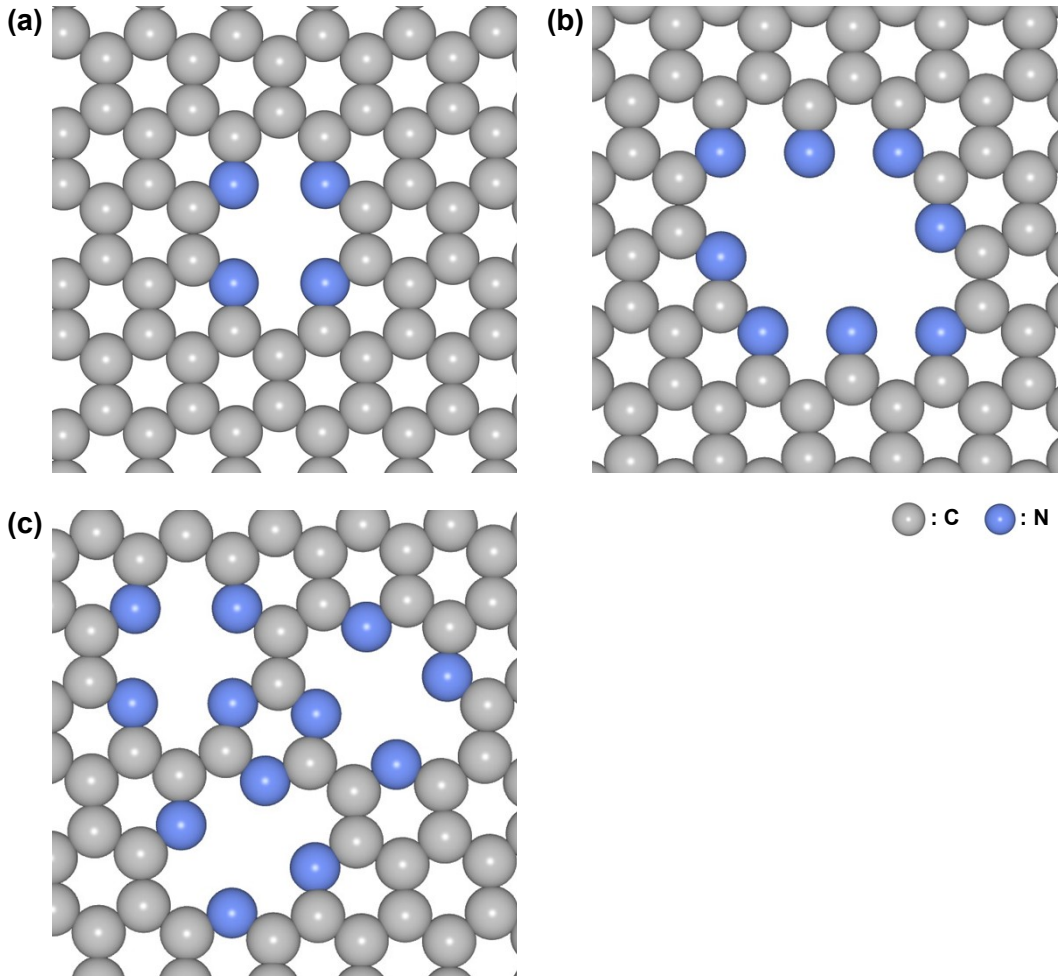

Figure S5. Illustration of base structures for (a) IrO_x/Ir SAC (or IrO_2 SAC), (b) m-Ir NP (or Ir_6 NP), and (c) l-Ir NP (or Ir_{12} NP).

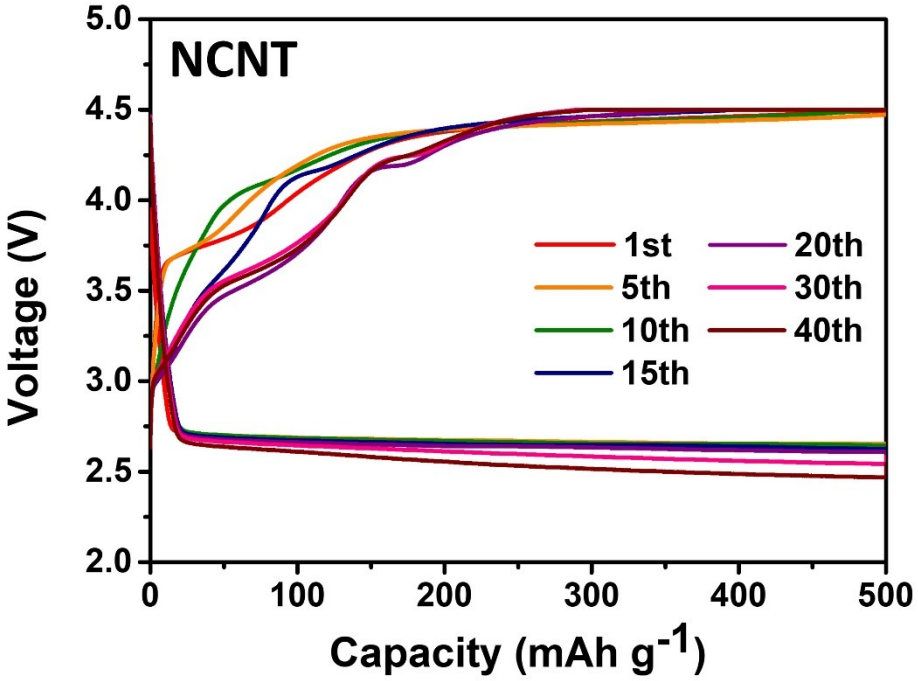

Figure S6. Cycling performance of Li-CO_2 cells employing NCNTs in the 2.3–4.5 V voltage window under the specific capacity limit of 500 mAh g_{carbon}^{-1}.

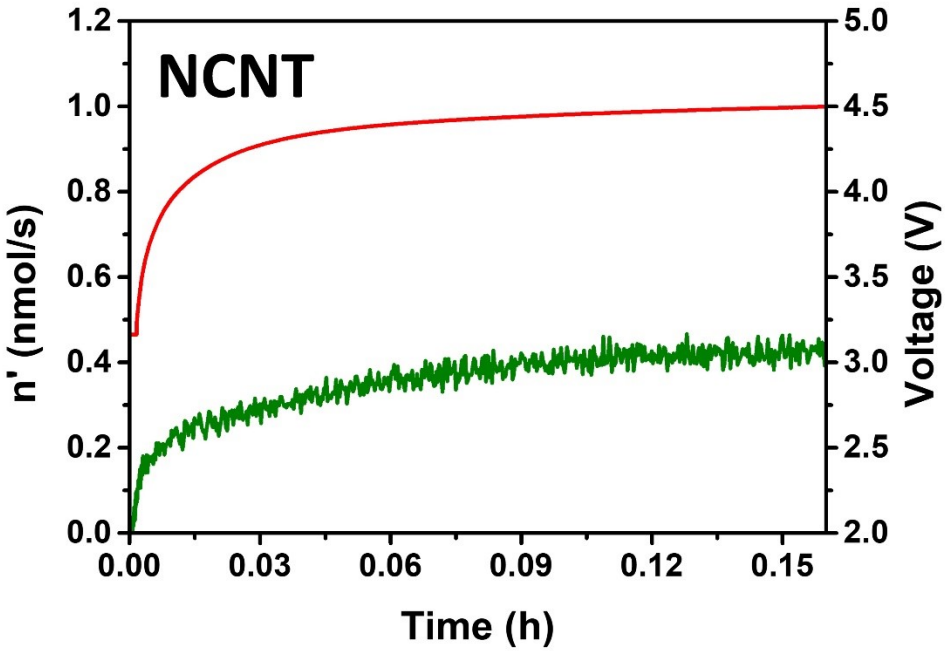

Figure S7. *In situ* DEMS results of the rate of evolution of CO_2 during charging in cells employing NCNTs.

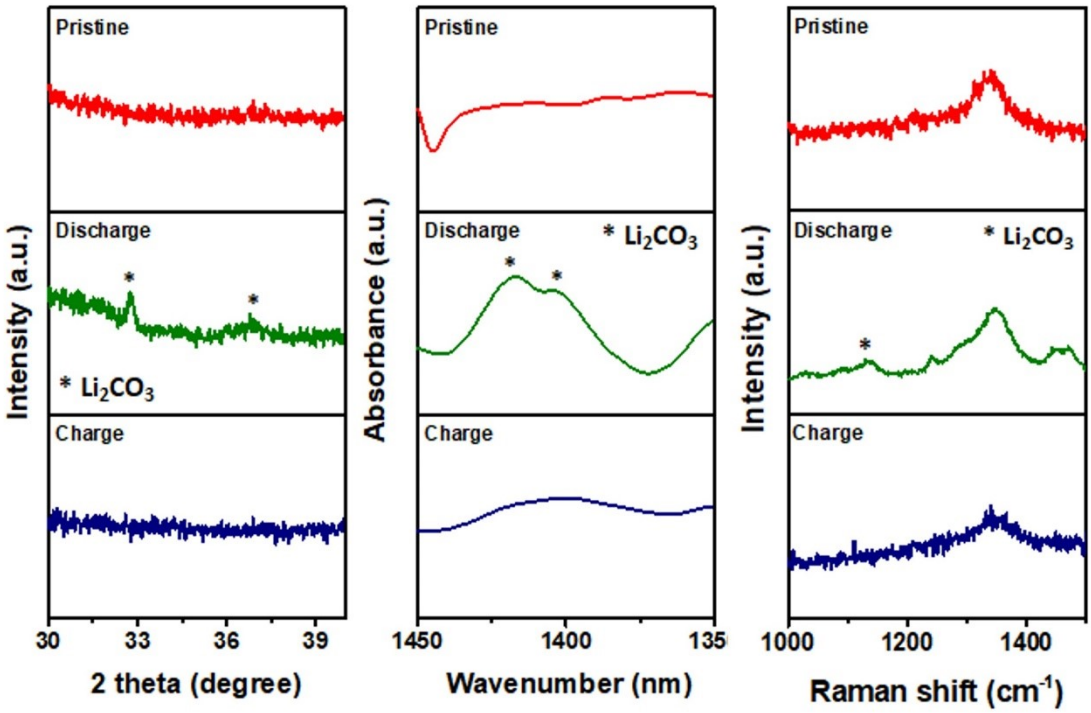

Figure S8. *Ex situ* measurements on carbon electrodes. XRD, FT-IR and Raman peaks obtained from discharged and charged electrodes of s-Ir/NCNT.

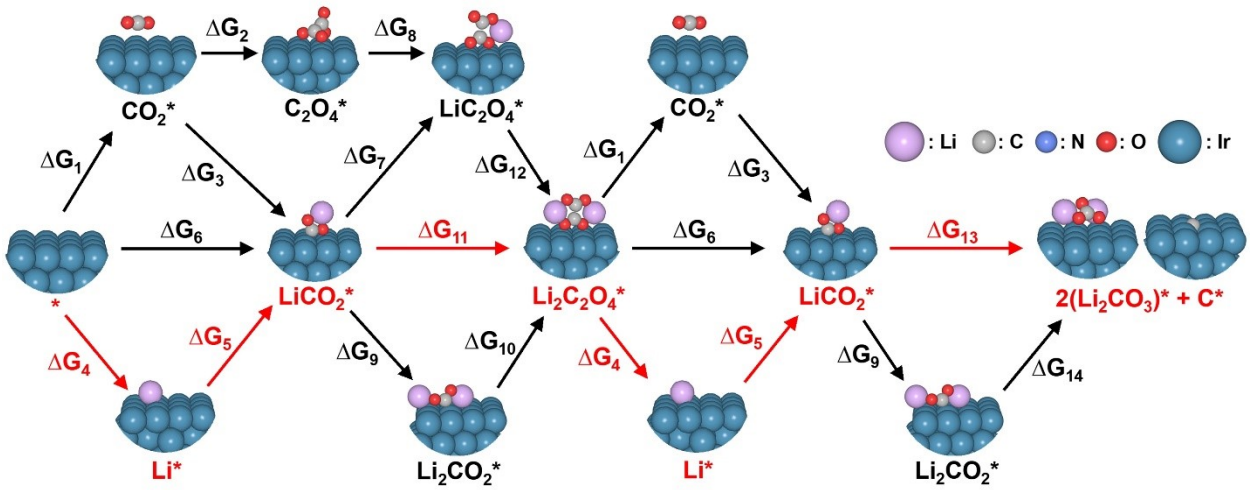

Figure S9. All the possible intermediates and reaction mechanisms for Li-CO_2 battery reaction, with the most feasible reaction pathway highlighted in red.

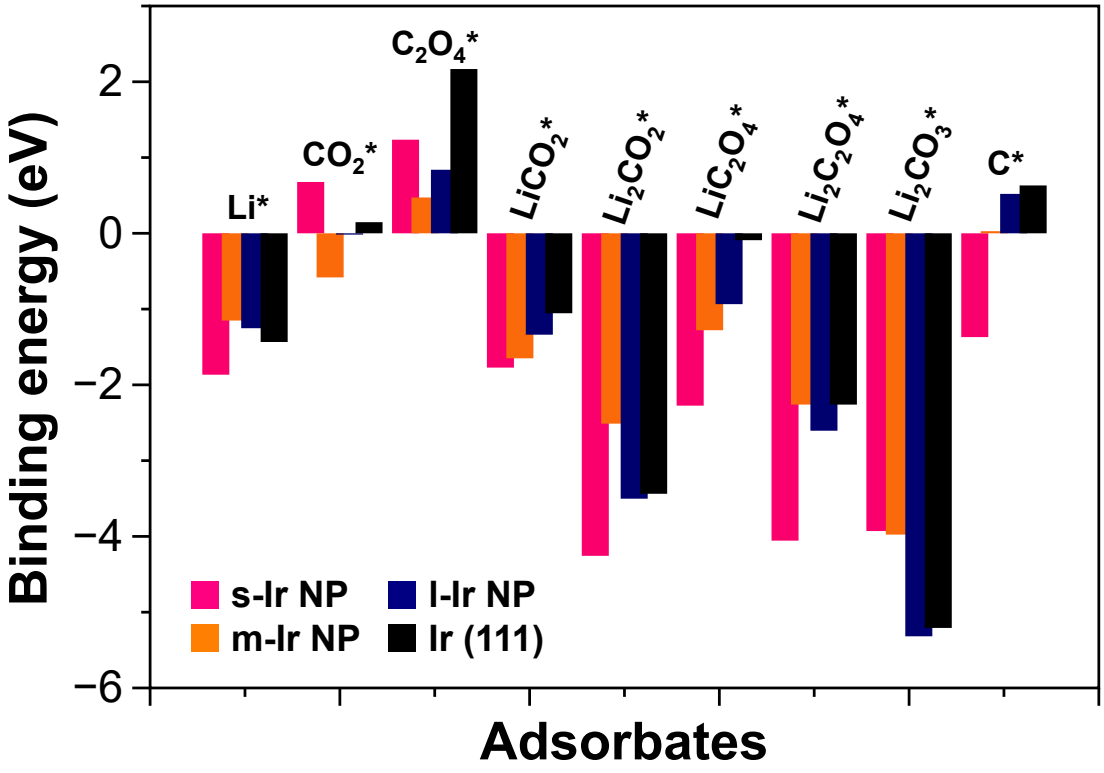

Figure S10. Binding energies of intermediates on the different Ir particle systems.

(a)

s-Ir/NCNT	Peak BE [eV]	Height CPS	Height ratio	Area CPS	Area ratio
$4f_{7/2}$ Ir^0	60.77	1261.63	1	1884.07	1
$4f_{5/2}$ Ir^0	63.78	1076.18	0.85	1469.38	0.78
$4f_{7/2}$ Ir^{4+}	62	660.95	0.52	1438.25	0.76
$4f_{5/2}$ Ir^{4+}	64.89	550.24	0.44	986.04	0.52

(b)

m-Ir/NCNT	Peak BE [eV]	Height CPS	Height ratio	Area CPS	Area ratio
$4f_{7/2}$ Ir^0	60.85	4758.32	1	5272.99	1
$4f_{5/2}$ Ir^0	63.8	3952.46	0.83	4738.88	0.9
$4f_{7/2}$ Ir^{4+}	61.98	1896.87	0.4	3153.06	0.6
$4f_{5/2}$ Ir^{4+}	64.88	1367.82	0.29	2273.66	0.43

(c)

l-Ir/NCNT	Peak BE [eV]	Height CPS	Height ratio	Area CPS	Area ratio
$4f_{7/2}$ Ir^0	60.78	9754.82	1	10856.96	1
$4f_{5/2}$ Ir^0	63.79	7689.14	0.79	10840.47	1
$4f_{7/2}$ Ir^{4+}	61.98	2927.77	0.3	3834.4	0.35
$4f_{5/2}$ Ir^{4+}	64.9	1654.65	0.17	1673.71	0.15

Table S1. Binding energies and relative integrated height and area from the Ir 4f XPS spectra of (a) s-Ir/NCNT, (b) m-Ir/NCNT, and (c) l-Ir/NCNT.

(eV)	ΔG_1	ΔG_2	ΔG_3*	ΔG_4*	ΔG_5	ΔG_6*	ΔG_7	ΔG_8*	ΔG_9*	ΔG_{10}	ΔG_{11}*	ΔG_{12}*	ΔG_{13}*	ΔG_{14}
IrO_2	0.678	0.558	-2.450	-1.866	0.094	-1.772	-0.502	-3.510	-2.484	0.201	-2.284	-1.782	-3.400	-0.916
Ir_6	-0.582	3.307	1.185	-1.151	-0.498	-1.650	0.371	-1.752	-0.862	0.252	-0.611	-0.981	-4.014	-3.152
Ir_{12}	-0.017	3.022	0.845	-1.253	-0.085	-1.338	0.403	-1.774	-2.165	0.897	-1.267	-1.670	-6.173	-4.008
Ir (111)	0.147	2.021	-1.202	-1.434	0.379	-1.055	0.964	-2.258	-2.382	1.177	-1.205	-2.170	-6.469	-4.086

Table S2. All the possible intermediates and reaction mechanisms for Li-CO_2 battery reaction and the most feasible reaction pathway in red color. * represents the ($Li^+ + e^-$) pair transfer step.